JOURNAL OF CHEMICAL INFORMATION AND MODELING

Article

pubs.acs.org/jcim

Molecular Dynamics Simulation and Site-Directed Mutagenesis of Alcohol Acyltransferase: A Proposed Mechanism of Catalysis

Luis Morales-Quintana, María Ximena Nuñez-Tobar, María Alejandra Moya-León, and Raúl Herrera*

Laboratorio de Fisiología Vegetal y Genética Molecular, Instituto de Biología Vegetal y Biotecnología, Universidad de Talca, Casilla 747, Talca, Chile 3465548

Supporting Information

ABSTRACT: Aroma in *Vasconcellea pubescens* fruit is determined by esters, which are the products of catalysis by alcohol acyltransferase (VpAAT1). VpAAT1 protein structure displayed the conserved HxxxD motif facing the solvent channel in the center of the structure. To gain insight into the role of these catalytic residues, kinetic and site-directed mutagenesis studies were carried out in VpAAT1 protein. Based on dead-end inhibition studies, the kinetic could be described in terms of a ternary complex mechanism with the H166 residue as the catalytic base. Kinetic results showed the lowest Km value for hexanoyl-CoA. Additionally, the most favorable predicted substrate orientation was observed for hexanoyl-CoA, showing a coincidence between kinetic studies and molecular docking analysis. Substitutions H166A, D170A, D170N, and D170E were evaluated in silico. The solvent channel in all mutant structures was lost, showing large differences with the native structure. Molecular docking and molecular dynamics simulations were able to describe unfavored energies for the interaction of the mutant proteins with different alcohols and acyl-CoAs. Additionally, in vitro site-directed mutagenesis of H166 and D170 in VpAAT1 induced a loss of activity, confirming the functional role of both residues for the activity, H166 being directly involved in catalysis.

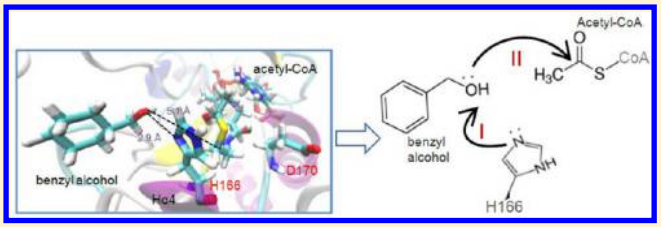

INTRODUCTION

Aroma is determined by a large number of volatile compounds and it is an important attribute of fruit quality. The final aroma of a particular fruit depends on the type of volatile produced and their relative concentrations. The biosynthesis of aroma in fruits is affected by several factors such as cultivar, ripening stage, and postharvest conditions.[1] Mountain papaya fruit (*Vasconcellea pubescens*) is characterized for its fruity and strong aroma which is determined mainly by esters and in lower proportion by alcohols.[2]

Esters are aroma-active compounds generated by esterification reactions between alcohols and acyl-CoAs, the reaction being catalyzed by alcohol acyltransferases (AAT; EC 2.3.1.84).[3,4] A gene encoding an AAT (VpAAT1) was isolated and characterized from ripe mountain papaya fruit.[5] VpAAT1 is a member of the BAHD superfamily.[5] The name BAHD was coined from the substrates of the first four enzymes of the family isolated from plants: benzylalcohol acetyl-, anthocyanin-*O*-hydroxy-cinnamoyl-, anthranilate-*N*-hydroxy-cinnamoyl/benzoyl-, and deacetylvindoline acetyltransferase.[6] The VpAAT1 belongs to subfamily III,[5] together with other AATs that participate in the synthesis of volatile compounds during ripening of climacteric fruits such as melon.[7] Although these acyltransferases show only low sequence similarities (15−30% identity) with each other, they share two highly conserved motifs, suggesting that they may have evolved from a common ancestor.

Members of the BAHD superfamily share the HxxxD motif, located in the middle of the protein sequence, which is highly conserved in both higher plants and yeasts. Substitution of histidine and aspartate residues from this motif by alanine causes the loss of enzyme function in vinorine synthase,[8] a member of the BAHD superfamily, distantly related to VpAAT1 and other fruit AATs.[4] We recently reported the structural model of VpAAT1 protein built by homology modeling.[9] This model was uploaded to Protein Model Data Base[10] assigned with code PM0079098. In silico studies showed that histidine and aspartic residues could be involved in the transfer of the acyl group from acyl-CoA toward the alcohol.[9]

Some members of the BAHD superfamily have been biochemically characterized.[6] To date, acyl-CoA-dependent acyltransferases have been shown to utilize one of two kinetically distinct mechanisms to catalyze acyl transfer, i.e., the ternary complex and the double-displacement mechanisms: (i) the acyl transfer catalyzed by chloramphenicol *O*-acetyltransferase (CAT; EC 2.3.1.28),[11] the histone acetyltransferase (HAT),[12] and the malonyl-CoA:anthocyanin 5-*O*-glucoside-6‴-*O*-malonyltransferase (Ss5MaT1)[13] operate through ternary complex mechanisms, which require both substrates and the enzyme to form a ternary complex before the direct acyl transfer from acyl-CoA to the substrate acceptor, without the formation of a covalent acyl-enzyme intermedi-

Received: July 11, 2013
Published: September 15, 2013

Table 1. Primers Used for Site-Directed Mutagenesis of VpAAT1[a]

enzyme	DNA sequence[b]	
H166A	forward	5′-TTTGCCCTTCGCTTGAAC**GCC**ACCATGAGTGATGCATC-3′
D170E	forward	5′-GAACCACACCATGAGT**GAG**GCATCTGGGCTTGTAC-3′

[a]The reverse primer is complementary to the forward primer. [b]Black underlined bases indicate the positions of nucleotide changes.

ate,[11−13] and (ii) the acyl transfer catalyzed by thiolase (acetyl-CoA:acetyl-CoA C-acetyltransferases, EC 2.3.1.9)[14] proceeds with a double displacement mechanism that involves the acyl transfer from acyl-CoA to an enzyme nucleophile (a cysteine residue) prior to transferring to the second substrate.[14] The roles of the active site amino acid residues of these kinetically established acyltransferases have also been studied in detail in terms of their three-dimensional structures.[12,13,15]

The different AATs that participate in the synthesis of volatile compounds during fruit ripening are functional and phylogenically distinct from the known acyl-CoA-dependent acyltransferases mentioned above, and their three-dimensional structures, kinetic, and catalytic mechanisms, as well as the role of active site residues, are not yet known.

Notwithstanding the knowledge generated in the past few years, there is still a limited understanding of the mechanisms controlling the synthesis of aroma volatiles. The interaction of AAT protein and their ligands is considered important to clarify the role of the active site residues. In this sense, the microarchitecture of the active sites and the role of His and Asp of HxxxD motif of these enzymes can be studied using computational biology (molecular docking and molecular dynamics simulations) and biochemical (determination of kinetic parameters and dead-end inhibition studies) tools.

METHODS

In silico Site-Directed Mutagenesis of VpAAT1. The structural model of VpAAT1 protein previously described[9] displayed the HxxxD motif facing to a solvent channel located in the center of the structure formed between the two protein domains. To gain insight about the mechanism of action of VpAAT1 and to clarify the participation of the histidine and aspartate residues on catalysis, the mutants H166A, D170A, D170E, and D170N were generated from VpAAT1 wild-type structural model. In addition, the S34A mutation was performed as a negative control as this residue is located far from the solvent channel and the active site. Structural refinements of the different mutants of VpAAT1 were accomplished by molecular dynamics simulations (MDS) and equilibration methods using Nano Molecular Dynamics (NAMD 2.7) software[16] and Chemistry of Harvard Molecular Modeling (CHARMM27) force field for lipids and proteins[17,18] along with the TIP3P model for water.[19] After an initial minimization, the system was subjected to a short molecular dynamics run in order to remove wrong contacts and to fill empty pockets. All backbone atoms were restrained using a harmonic force constant of 5 kcal mol^{-1} $Å^{-2}$. All MDS were done using a time step of 1 fs, the structure obtained was embedded into a periodic boundary conditions (PBC) box (92 Å × 86 Å × 94 Å) at 300 K. Under these conditions, a 1 ns MDS was performed using NAMD v2.7 program.

Molecular Docking of Different VpAAT1 Mutants. Docking studies were performed to predict the putative modification of binding mode of a group of three different acyl-CoAs (acetyl-CoA, butanoyl-CoA, and Hexanoyl-CoA) and four different alcohols (ethanol, butanol, hexanol, and benzyl alcohol) with mutant variants of the structural model of VpAAT1. For this purpose, two different docking investigations using the Internal Coordinate Mechanics (ICM) program[20] (www.molsoft.com) were carried out. The active site used was the solvent channel of VpAAT1 structure previously described.[9]

The first docking was performed with acyl-CoA as acyl donor bound to the different mutant variants of VpAAT1. The other substrate, an alcohol, was used on the second docking. In order to verify that the order of entrance of ligands has no significant effect on the stability of the final complex, docking studies were also performed in reverse order reaching the same results, as it has been reported in the work of Morales-Quintana et al.[9] In each case, 10 different docking arrangements were produced. The conformations obtained as result of rigid-body docking were sorted by total binding energy. The result of rigid-body docking was optimized by flexible docking. Statistical analyses were performed using Statgraphic Plus v. 4.0, based on ANOVA and mean comparisons by Tukey HSD test, $P = 0.05$.

Molecular Dynamics Simulations (MDS). Molecular dynamics of substrates, alcohol, and acyl-CoA, inside the active site of each VpAAT1 mutant was studied by using NAMD 2.7[16] and CHARMM27.[17,18] The initial coordinates for MD calculations were taken from the docking experiments. TIP3P water molecules were added (the dimensions of each water box were 92 Å × 86 Å × 94 Å approximately, which ensured covering the entire surface of the complexes), and the systems were neutralized by adding KCl counterions to balance the net charges of the system. The systems were minimized and pre-equilibrated using the relaxation routine implemented to relax the initial models as described previously.[9] After that, a first 1 ns long equilibration MD simulation was performed on each complex system, which was followed by a 5 ns long MD simulation. In each case, two different MD simulations were produced. Paramchem[21] was used to provide and check the necessary force field parameters for the ligands. During MD simulations, the equations of motion were integrated with a 1 fs time step in the *NVT* ensemble. The van der Waals cutoff was set to 12 Å, and the temperature was maintained at 300 K. Data were collected every 1 ps during the MD runs. Visualization of protein−ligand complexes and MD trajectory analysis were carried out with the VMD software.[22]

In vitro Mutagenesis of VpAAT1 and Protein Expression and Purification. Specific mutations were performed using the QuikChange II kit (Stratagene) with the pYES2.1-VpAAT1 plasmid as a template following the instructions provided by the manufacturer. The mutagenic primers used are described in Table 1. To confirm the successful introduction of mutations, three different plasmids for each mutant were sequenced using the services of Macrogen Inc. (Seoul, Korea).

Wild-type and two mutant variants of VpAAT1 (H166A and D170E) were cloned into pYES2.1 TOPO-TA cloning vector containing a C-terminal polyhistidine tag following the instructions provided by the manufacturer (Invitrogen) according to the method of Balbontín et al.[5] The variants were cloned in *Escherichia coli* TOP 10 One Shot (Invitrogen)

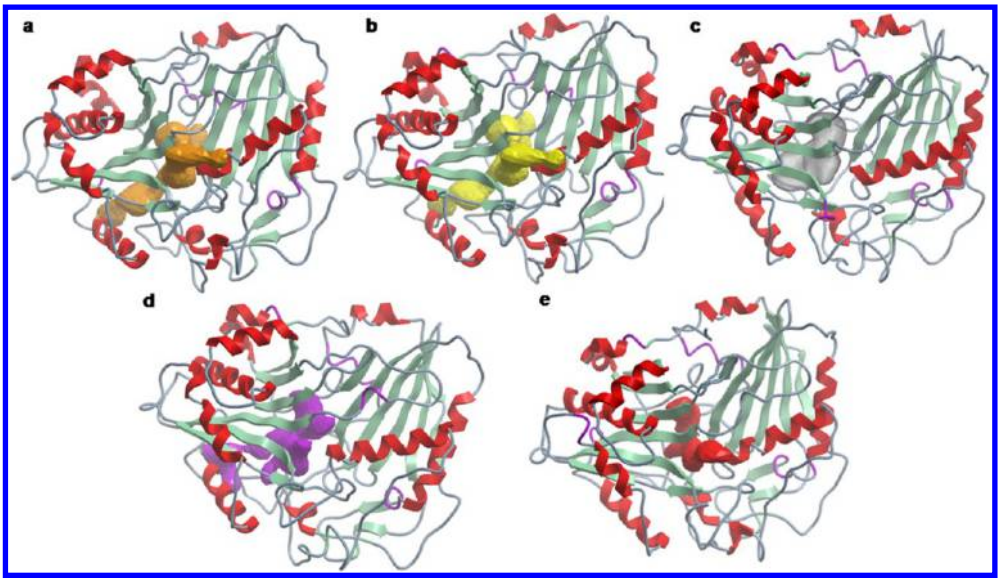

Figure 1. Pocket surfaces of different VpAAT1 mutants. A view of (a) S34A, (b) H166A, (c) D170A, (d) D170N, and (e) D170E mutant protein models. No significant changes in the solvent channel structure were observed in parts a and b, while in parts c−e, the structure of the solvent channel was dramatically modified.

and sequenced by Macrogen Inc. (Seoul, Korea). Once the right orientation of insert was confirmed, the construct was used to transform the *Saccharomyces cerevisiae* cell line INVSc1. Transformed yeasts were grown at 30 °C in selective medium (SC-U) with 2% galactose as inducer of the expression of recombinant protein, with constant stirring until OD_{600} of the culture reached <1.

The purification of different mutant variants of VpAAT1 recombinant protein was carried out according to the method of El-Sharkawy et al.[7] with modifications.[5,9] The different recombinant proteins were purified through a Talon Metal Affinity column, designed to purify polyhistidine-tagged proteins, according to the manufacturer's protocol. Proteins were quantified according to the work of Bradford[23] and visualized through 10% SDS-PAGE gels.

Assay of AAT Activity, Kinetic Parameters, and Inhibitory Studies. AAT activity of recombinant wild-type and mutant variants of VpAAT1 were quantified by its ability to convert alcohols and acyl-CoAs into the corresponding ester[24] as reported earlier.[5,25] Briefly, AAT activity was assayed in the presence of 2 mM alcohols and 250 μM acyl-CoAs in 50 mM Tris-HCl (pH 7.5) buffer containing 10% (v/v) glycerol and 1 mM dithiothreitol (DTT).[5,7,9] The reaction was initiated by addition of 35 μg purified protein and incubated at 30 °C for 2.5 h. After stopping the reaction the volatiles produced were adsorbed onto solid-phase microextraction (SPME) fibers (PDMS/DVB). Volatiles were separated and quantified by gas chromatography (Agilent Technologies, GC system 7890A) coupled to a mass spectrum (Agilent Technologies, MSD 5975C). Calibration curves were prepared for benzyl acetate, butyl acetate, and hexyl acetate using 1,2-dichlorobenzene as internal control. AAT enzyme activity was expressed as picomoles per hour per milligram of protein. Determinations were performed in triplicate and expressed as mean ± standard error (SE).

For determination of K_M and V_{max} values, standard assay mixtures were prepared. Michaelis−Menten saturation curves were built using substrate concentrations between 0 and 8 mM for alcohols and between 0 and 4 mM for acyl-CoAs. The K_M and V_{max} values were calculated from Nonlinear least-squares data fitting (NLSF) in Excel spreadsheets according to the work of Kemmer and Keller,[26] determinations were performed in triplicate and expressed as mean ± SE. Inhibitory studies were also performed with coenzyme-A (CoA-SH) (250 μM) with acetyl-CoA and hexanol as alcohol; the K_M and V_{max} values were calculated from Hanes−Woolf plot to graphically illustrate the differences of K_M and V_{max}.

RESULTS AND DISCUSSION

In silico Site-Directed Mutagenesis of VpAAT1. *Structure of Different VpAAT1 Mutants.* Multiple protein sequence alignment revealed that proteins in the BAHD family proteins share a sequence identity of 25−34%[27] and contain 19 amino acid residues that are absolutely conserved.[27,28] Two of them are the His and Asp residues of the HxxxD motif. The importance of His and Asp of the HxxxD motif has been demonstrated for other members of the BAHD family by chemical modification and mutagenesis experiments.[8,13]

VpAAT1 was previously modeled,[9,29] and therefore, in silico site-directed mutagenesis was performed to better understand the catalytic mechanism. Five mutants H166A, D170A, D170E, D170N, and S34A were in silico generated and evaluated. In addition, previous results indicate that the structure of the solvent channel of AAT protein is crucial for activity,[28,29] and therefore, the solvent channel of each mutant protein were evaluated.

First, when both VpAAT1-Wt and VpAAT1 mutants 3D proteins models were superimposed (SI-2), their root-mean-square deviation (RMSD) values indicated a good overall structural alignment (RMSD value of the backbone of whole structures is 0.65 Å, and RMSD of the active site motif is 0.22 Å). The protein displayed similar 3D structures with β-sheets and α-helices in similar arrangement and distribution, showing the catalytic residues (H166 and D170 residues or the corresponding substitution) exposed to the solvent channel of each protein in equal orientation.

Solvent Channels of Different VpAAT1 Mutants. Major differences in the mutants were shown in the shape and size of

dx.doi.org/10.1021/ci400409s | J. Chem. Inf. Model. 2013, 53, 2689−2700

the solvent channels of the protein models may be appreciated (Figure 1). The solvent channel of S34A mutant protein is similar to the channel described previously for VpAAT1 protein, with the residues required for catalytic action oriented to the central cavity of the channel (Figure 1a). Also, no change was determined in the solvent channel structure of H166A mutant compared to wild type (Figure 1b). The shape and size of the solvent channels of both mutant proteins are equal (Table 2). In wild type protein the solvent channel was

Table 2. Volumes and Areas of Different Solvent Channel Shown in Figure 1 for Each VpAAT1 Mutant

protein model	volume (Å^3)	area (Å^2)
wild type	1085.7	1011.2
S34A	1081.2	1009.3
H166A	1081.1	1009.1
D170A	611.8	503.6
D170E	385.7	433.2
D170N	702.6	741.9

previously characterized[29] and the volume with the area similar to S34A and H166A protein mutant models. On the contrary, in D170A, D170N, and D170E mutant proteins, the solvent channels differ from the wild type protein, the pockets are smaller, but also the channel is not formed (Figure 1c–e); additionally, a lower volume of the pockets was determined (Table 2). In addition, in the wild-type[9] and all mutants' protein, the side chain orientation of Asp170 is such that it is not involved in hydrogen bonding with His166.[9] Asp170 is rather involved in the formation of a salt bridge with the conserved Arg294, which is most likely to be important for the maintenance of the geometry of the active site, similar to the observations in the structure of vinorine synthase.[28] In D170A protein model the alanine is not able to form the salt bridge with Arg294, similar to the asparagine residue in D170N protein model, and the lack of this salt bridge destabilizes the region of the active site producing the loss of channel structure. Unexpectedly, in the D170E protein model the glutamate could established a salt bridge with the conserved Arg294 (Figure 2); however, this interaction is unstable as described by MDS. During the molecular dynamics simulation, it is clearly shown that the salt bridge is lost (Figure 2, arrow III), causing the reorientation of the side chains of the Arg residue that modifies one of the entrances to the solvent channel (Figure 2c). In the case of S34A and H166A protein models, no differences in the solvent channel structure were observed in comparison to the wild type because the two proteins have the aspartate residue (D170) (Figure 1) and the salt bridge is present.

Ligand Binding Analysis. The models of VpAAT1 mutants were used to study protein–ligand conformations by automatic docking for seven substrates (three acyl-CoAs and four alcohols). Substrates were chosen based on the data of activity and affinity energy previously reported[9] and are used by the enzyme to generate the most abundant ester found in the fruit. As shown in the Supporting Information (SI-1), for all ligands tested the negative energies indicate a favorable interaction between the proteins and the ligands with only minor differences observed between the native enzyme and the mutants assessed. However, a less interaction energies were observed in H166A mutant protein for the interaction with acyl-CoAs. The strongest binding interaction was found between each the D170N, D170E, and S34A mutant and hexanoyl-CoA and with acetyl-CoA in the case of H166A and D170A mutants.

Ternary complexes were obtained building first the complex acyl-CoA_protein (VpAAT1 mutants) and then incorporating the alcohol as described earlier.[9] The interaction of wild type protein with different substrates was already described,[9] and the best affinity energy was for the acetyl-CoA_benzyl-alcohol_-wild type complex with −266.3 kcal mol^{-1}. In addition, the model revealed that His166 is protonated at the ε nitrogen, which forms a hydrogen bond with the hydroxyl group of acetyl-CoA, and the distance between the carboxylic group of Asp170 and the hydroxyl group of benzyl alcohol was 2.73 Å, in an adequate position to stabilize this substrate through a hydrogen bond.[9] Interestingly, the complexes of acyl-CoA_alcohol_H166A-protein show a similar binding position for the alcohol (which interacts with Asp170) compared to the wild type enzyme, although acyl-CoA molecule differs in its orientation in the solvent channel and the distance between the hydroxyl group of acyl-CoA and Nδ of His166 is longer (Figure 3).

In the acetyl-CoA_benzyl alcohol_H166A complex, A166 cannot form a hydrogen bond with the hydroxyl group of acetyl-CoA (Figure 3b) and the substrate is located 12.3 Å from the alanine residue. Additionally, the distance between the carboxylic group of D170 and the hydroxyl group of benzyl alcohol was 5.2 Å, considered as an unfavorable position to stabilize this substrate through the hydrogen bond. Similar long distances between H166 and the reactive bond of acetyl-CoA were found in all mutant proteins (data not shown). In the case of S34A (negative control), no significant differences in the position of the two substrates, acetyl-CoA and benzyl alcohol, and the two catalytic residues were found with respect to the wild-type enzyme (Figure 3a).[9]

For D170A and D170N, the acetyl-CoA with respect to nitrogen δ of His from motif HxxxD was oriented at a similar unfavorable distance (between 10.5 and 13.7 Å) and the alcohol is also located far from and at an unfavorable position to A170 and N170 residues, respectively (Figure 3c and d). In D170E a longer distance was observed for benzyl alcohol from Glu170 and for acetyl-CoA with respect to H166 residue. Interestingly, as major changes are displayed in the solvent channel in the mutants, the entrance of both ligands to the channel is through the corresponding entrance of acyl-CoA substrate within the native enzyme (Figure 2e). Thus, the main difference between acetyl-CoA_benzyl alcohol_D170E complex and acetyl-CoA_-benzyl alcohol_wild type complex is the location of the alcohol into the solvent channel and the distance of the ligands with residues E170 in the wild-type or D170 in the mutant (Figure 3e). This is produced by the conformational change of the solvent channel structure due to the loss of interaction between D170E and Arg294 residues (Figure 2).

Affinity Energy Analysis. The imidazole Nδ of His166 plays an essential part in the proposed general base mechanism of VpAAT1.[9] This mechanism is still in place in the S34A mutant protein that was used as negative control. However it is not possible to find residues in favorable orientation in the case of the other four mutants, and therefore, the esterification reaction cannot take place (Figure 3).

Table 3 shows the affinity energy of the interaction for different mutant proteins with a series of substrates. The energy values of H166A mutant protein are unfavored compared to the native VpAAT1 protein although the solvent channel has no structural change (Figure 1b). This indicates that the His

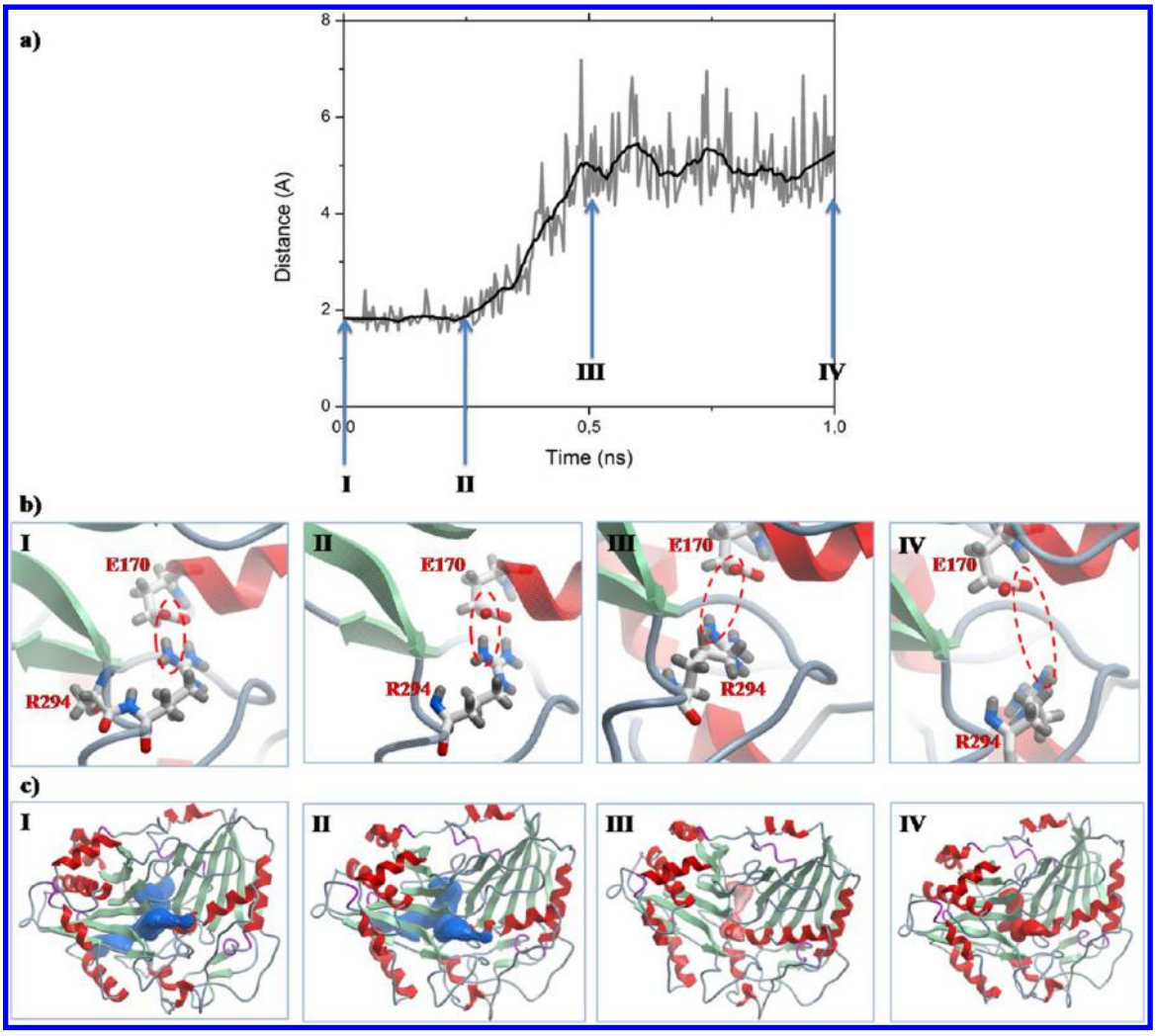

Figure 2. Analysis of the solvent channel structure and stability of the interaction between D170 and R294 residues during the MDS in D170E mutant protein models. (a) Distance between Arg294 and Glu170 residues along the molecular dynamics (MD) trajectory. Four different images were taken during the MDS at 0, 0.25, 0.5, and 1 ns (blue arrows) and shown in parts b and c. (b) Images taken during the MDS at 0, 0.25, 0.5, and 1 ns showing the interaction of Arg294 and Glu170, showing the instability of the salt bridge formed between these two residues. (c) Views of the protein model and the solvent channel during the MD trajectory. During the first 0.25 ns of simulation, the solvent channel remains intact (points I and II); however after that, the side chain of Arg294 residue reorients and moves away from Glu170 residue, which produces the rupture of the salt bridge and consequently the loss of the solvent channel structure (points III and IV).

residue is involved in the catalysis and not in the solvent channel structure or the enzyme structure. In the case of D170A and D170N complexes were also determined and were unfavored, similarly to the case of H166A. Both D170 mutants present major structural changes in the solvent channel (Figure 1c and d), which could explain the unfavored interaction of the enzyme with the substrates and predicts a low enzymatic activity. No change in the interaction energy of the negative control (S34A mutant) with substrates was observed compared to native protein and the structure of the solvent channel is similar to the wild-type enzyme (Figure 1a). Interestingly, the D170E mutant protein showed a decrease in interaction energy with all substrates tested, except for ethanol and acetyl-CoA.

Therefore, our data indicate that it is unlikely that these two residues (His166 and D170) function as a dyad in the catalysis as proposed for human carnitine acetyltransferase.[30] On the contrary, Asp170 does not appear to have a direct role in catalysis as it has been proposed for several other acyltransferases,[8,13,30] and it is most likely to have a structural importance.

MD Simulations. VpAAT1 enzyme has a strong activity toward the esterification of benzyl alcohol and acetyl-CoA to produce benzyl acetate and in contrast it does not produce ethyl acetate (from ethanol and acetyl-CoA as substrates).[5] The protein−substrate interaction of these substrates with the active site of VpAAT1 wild-type protein and the different mutants was studied using MD simulations.

In the wild type simulation with benzyl alcohol and acetyl-CoA as substrates, at the beginning of the molecular dynamics the hydroxyl group of benzyl alcohol interacts first with the carboxylic group of D170 residue (Figure 4a, black line). At the same time, H166 residue is far from benzyl alcohol and close to the carbonyl group of acetyl-CoA. However during the MD simulation the distance between nitrogen δ of H166 and the hydroxyl group of benzyl alcohol decreases at around 2 ns (Figure 4a, purple line). It can be noticed that H166 does not move far from acetyl-CoA (Figure 4a, blue line) while benzyl alcohol reorients toward the H166. However, the displacement of the alcohol from D170 to H166 is not direct and it is facilitated by a serine residue (S370). This has been recently

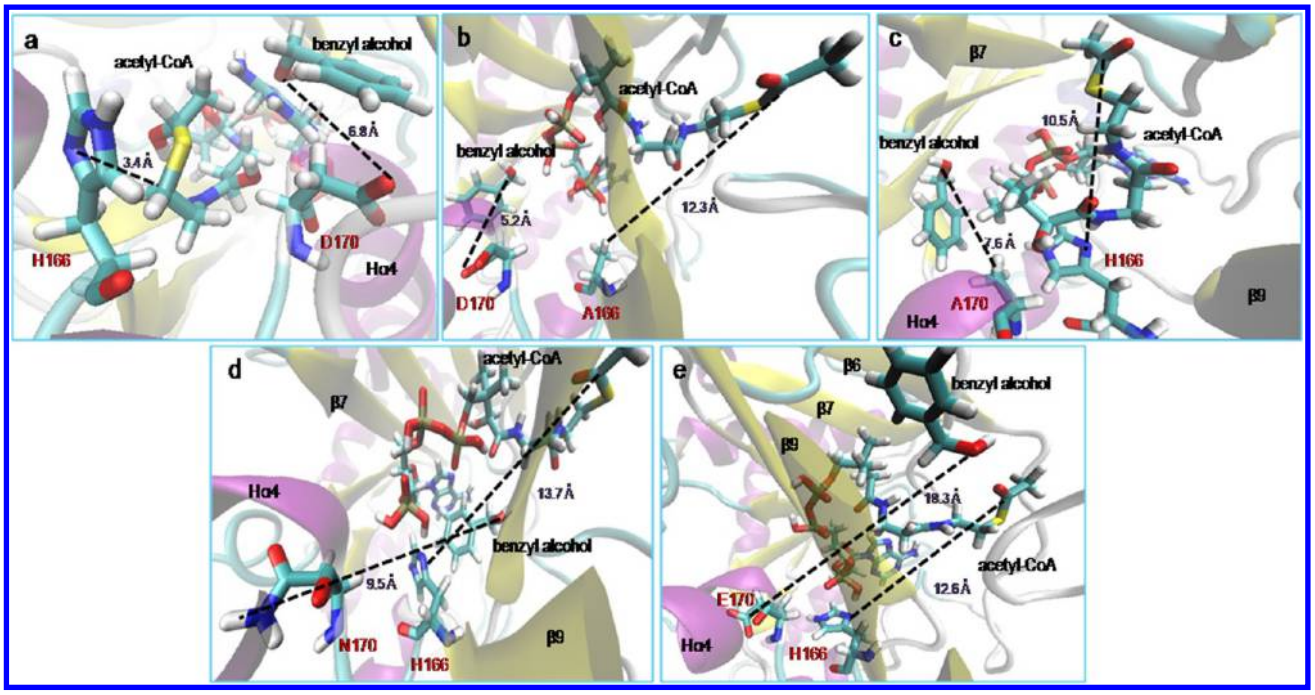

Figure 3. Spatial distribution of substrates in the active site of each mutant protein−ligand model using benzyl alcohol and acetyl-CoA as substrates. The pair of substrates was chosen based on the VpAAT1 wild-type protein.[9] A detailed view of the active sites of S34A (a), H166A (b), D170A (c), D170N (d), and D170E (e) mutant proteins is shown. In parts a and b, the residues show a similar orientation to the wild type enzyme,[9] with short distances between H166 residue and acetyl-CoA, and D170 with benzyl alcohol. While in parts c−e, the substrates are far to residues of HxxxD motif. Representative image after 10 different docking arrangements.

described by Galaz et al.[31] in *Cucumis melo* CmAAT1 enzyme with a crucial role of the serine residue in the formation of H163−N_{δ}-alcohol-acyl-CoA complex. The dynamics show the approaching of alcohol and the shift of its hydroxyl group toward the carbonyl of acyl-CoA. In VpAAT1, S370, located in β strand 11 and oriented toward the channel solvent, interacts with benzyl alcohol and acetyl-CoA as revealed during MD: at 0.5 ns the distance from benzyl alcohol to D170 increases to around 10 Å (Figure 4a, black line) while the distance of the benzyl alcohol toward the S370 decreases (Figure 4a, red line). Interestingly, S370 residue does not interact with acetyl-CoA, and during the entire molecular simulation, the distance from the hydroxyl group of S370 to the carbonyl group of acetyl-CoA is between 6 and 8 Å (data not shown).

In the case of acetyl-CoA_ethanol_wild type, at the beginning of molecular docking simulation, ethanol interacts with D170 and acetyl-CoA with H166.[9] However, during MD simulation, the orientation of the ethanol changes moving away from D170 (to around 5.5 Å) (Figure 4b, black line) and also from H166 (9 Å) (Figure 4b, purple line). Additionally, the stability of substrates in the solvent channel is neither favorable for ethanol with an RMSD value of around 20 Å (Figure 5a, gray line) nor for acetyl-CoA as cosubstrate. The stability of benzyl alcohol in the best complex is around 0.4 Å (Figure 5a, black line) with acetyl-CoA as cosubstrate. Interestingly, the substrate acetyl-CoAs in the two MD trajectories showed low RMSD values, around 1.5 Å for acetyl-CoA with benzyl alcohol as cosubstrate (Figure 5b, gray line) and 2.5 Å for acetyl-CoA when ethanol is the cosubstrate (Figure 5b, black line).

In His166A mutant, the substrates were badly oriented and also located too far from the catalytic residues along the entire MD simulation (Figure 6a): Ala166 is far from benzyl alcohol (Figure 6a, purple line), and benzyl alcohol is far from both A166 and D170.

MD simulations presented here explains the importance of histidine as a catalytic residue. In this sense, a significant decrease in the distance between H166 and benzyl alcohol at the middle of the simulation was observed. The minimum distance of 3.1 Å could reflect the direct interaction between the substrate and the residue (Figure 4a, purple line).

For the Asp170 mutants in all MD simulations, the substrates were wrongly oriented (Figure 3c−e). The hydroxyl group of benzyl alcohol does not interact with the side group of the residue in position 170 (Figure 3). Interestingly, His166 residue in all Asp170 mutants is far from benzyl alcohol at the beginning of the MDS and close to the carbonyl group of acetyl-CoA, similar to wild type; however during the MD simulation, the distance between nitrogen δ of His166 and the hydroxyl group of benzyl alcohol does not decrease, in D170A the distance between nitrogen δ of His and the hydroxyl group of benzyl alcohol is around 9 Å (Figure 6b, purple line). The alcohol is not close to H166 in the solvent channel even when S370 residue is present in the solvent channel as in the wild type. However, the position of S370 residue is different and the alcohol is far to this residue due to the modifications made on the solvent channel after the mutation of D170A (Figure 6b, red line). When the Asp170 residue was mutated to Asn or Glu, the molecular dynamics trajectory was similar to that described previously in Figures 5 and 6 for D170A mutant (data not shown).

Kinetic Analyses. Kinetic properties of the recombinant VpAAT1 enzyme were determined to validate in silico measurements. The K_M and V_{max} values were determined for four different alcohols using acetyl-CoA as cosubstrate at saturating concentration (2.5 mM), and for three acyl-CoAs

Table 3. Affinity Energies for the Different Acyl-CoA_Alcohol_VpAAT1-Mutant Complexes[e]

substrates		wild-type		H166A		D170A		D170N		D170E		S34A	
acyl-CoA	alcohol	affinity energy (kcal mol^{-1})[f]	RMSD (Å)[g]	affinity energy (kcal mol^{-1})	RMSD (Å)[g]	affinity energy (kcal mol^{-1})	RMSD (Å)[g]	affinity energy (kcal mol^{-1})	RMSD (Å)[g]	affinity energy (kcal mol^{-1})	RMSD (Å)[g]	affinity energy (kcal mol^{-1})	RMSD (Å)[g]
acetyl-CoA	benzyl alcohol	−266.3[a]	2.4	−43.2 [c]	0.5	−50.1[c]	1.1	−48.2[c]	2.5	−149.1[b]	0.5	−265.1[a]	1.5
	hexanol	−222.9[a]	4.1	−46.2 [c]	4.9	−53.3[c]	0.7	−49.9[c]	4.8	−130.9[b]	5.1	−224.0[a]	3.2
	ethanol	−73.3[a]	4.4	−27.9[c]	1.1	−56.9[b]	1.9	−52.1[b]	9.3	−90.3[a]	2.6	−70.1[a]	5.2
butanoyl-CoA	ethanol	−230.9[a]	5.7	−28.7 [d]	1.4	−22.9 [d]	1.9	−54.8[c]	2.1	−170.9[b]	4.2	−232.3[a]	4.9
hexanoyl-CoA	ethanol	−250.2[a]	1.9	−33.2[c]	1.1	−32.4[c]	1.6	−45.7 [c]	2.5	−159.2[b]	2.1	−247.9[a]	0.8

[e]Different superscripted letters indicate significant differences in each mutant enzyme with respect to native enzyme within the same row for a given compound in each pair of substrate (Tukey HSD test, $P = 0.05$). [f]Affinity energies and RMSD values of VpAAT1 wild type enzyme were obtained from ref 9. [g]RMS deviation was calculated for the backbone (Cα, C, N) atoms.

using benzyl alcohol or hexanol as cosubstrates at saturating concentration (4 mM; Table 4). Lower K_M values were calculated for acyl-CoAs than for the alcohols. A trend was observed, wherein the K_M values for the alcohols decrease as the length of the acyl moiety increases, and similarly, the K_M values for the acyl-CoAs decrease as the acyl-CoA moiety increases. Interestingly, a low K_M value (79.7 μM) was found for acetyl-CoA using benzyl alcohol as cosubstrate which is coincident with the best substrates recorded for VpAAT1.[5] The VpATT1 enzyme displays a better affinity for benzyl alcohol (K_M 127.9 μM) than for butanol (K_M 186 μM). The data is in agreement with the activity reported by Balbontín et al.[5] for VpAAT1 wild-type recombinant enzyme with different alcohols. This property is also similar to those of CmAAT1 from *Cucumis melo*[32] and FaAAT1 from Cv. Oso Grande strawberry fruits.[33] On the contrary, a higher AAT activity was reported in banana AAT toward butanol, amyl-, and isoamyl alcohols than to hexanol.[34]

This higher specificity of the enzyme for the acyl moiety seems to indicate that the alcohol is the rate-limiting factor in the formation of most esters in mountain papaya fruit. Results obtained here are also consistent with those reported from banAAT1 of banana.[35] As was described for the alcohols, the lengthening of the acyl-CoA carbon chain is also correlated with higher substrate specificity (when hexanol was used as the cosubstrate).

In vitro Mutagenesis of VpAAT1, Enzymatic Activity Assay. Recently, we described that VpAAT1 recombinant protein was able to use different alcohols and acyl-CoAs as substrates for the synthesis of esters.[5] Additionally, we showed that the binding complex energies between VpAAT1 protein and its different substrates (acyl-CoAs and alcohols) were significantly different.[9] A good correlation was observed between VpAAT1 activity recorded for the recombinant protein and the affinity energy determined for each protein−ligand complex: a higher VpAAT1 activity and the affinity was measured when the complex showed higher stability (lower affinity energy).[5,9]

To gain insight about VpAAT1 mechanism of action and as complement to the in silico studies, site-directed mutations were designed in H166 and D170 residues. The mutant H166A and D170E proteins exhibited a complete loss of enzyme activity tested against a group of substrates (data not shown). These mutagenesis studies confirmed that H166 and D170 residues are indispensable for the acyltransferase activity of VpAAT1.

To probe the involvement of functional amino acid residues in the VpAAT1 mechanism on the basis of the general acid/base catalysis proposed above, in silico mutagenesis were designed and then tested in vitro. The in vitro mutagenesis studies revealed that the substitution of His-166 by Ala was accompanied by 99.8% activity loss with 0.01 nmol h^{-1} mL^{-1} while the wild-type protein showed the high activity with 20.46 nmol h^{-1} mL^{-1} to benzyl acetate ester;[5] additionally, for hexyl acetate the activity showed traces levels with less 0.0001 nmol h^{-1} mL^{-1} of ester production. Meanwhile when tested with substrates to produce ethyl acetate, ethyl butanoate and ethyl hexanoate did not show activity. In comparison, molecular docking with the H166A structural model revealed that the affinity energies were less favorable than for the native enzyme (Table 3). Additionally, MD simulation showed that His166 can form a hydrogen bond with the substrate (Figure 4, purple and blue lines). This strongly suggests that the His166 residue acts as a general base in the ternary "enzyme−substrate"

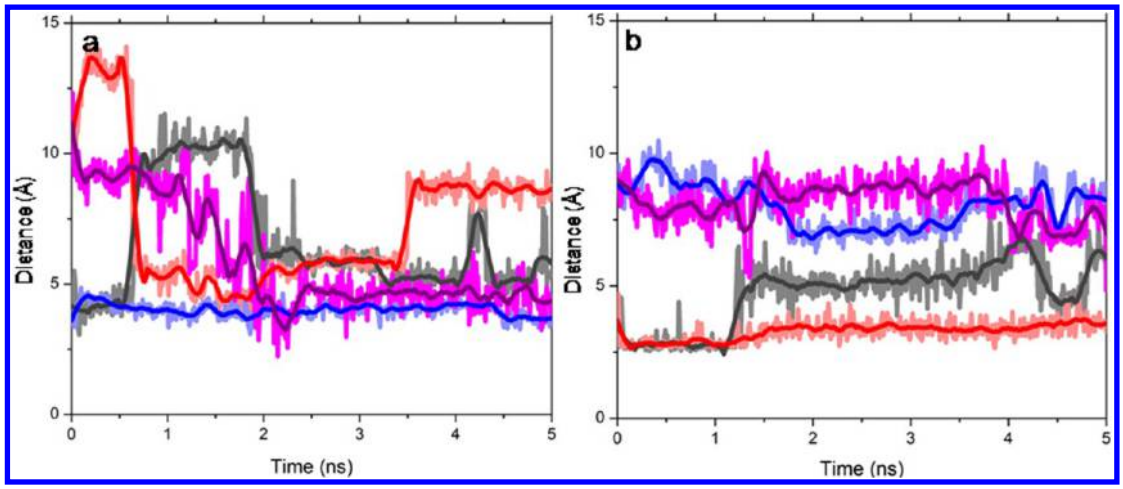

Figure 4. Distance between ligands and active site residues during MD simulation of native protein. The central line represents 30 FFT smoothing. The purple, red, and black lines show the distance from His166, Ser370. and Asp170 to the alcohol, respectively, and the blue line shows the distance between His166 and acetyl-CoA. (a) Best substrate-VpAAT1 wild type protein complex using benzyl alcohol and acetyl-CoA as substrates. A significant decrease in the distance between H166 and benzyl alcohol at the middle of the simulation (2.2 ns) was observed (purple line). The minimum distance of 2.4 Å could facilitate a direct interaction between the substrate and the H166 residue, this favored by Ser370 residue (red line). (b) Worst substrate−protein complex using ethanol and acetyl-CoA as substrates. Ethanol position changes at the beginning of the MD trajectory. The distance between ethanol and D170 (black line) grows to around 5.5 Å. The minimum distance of 9.0 Å between ethanol and H166 (purple line) does not facilitate a direct interaction between the substrate and the H166 residue. Representative trajectory after 2 different MD simulations.

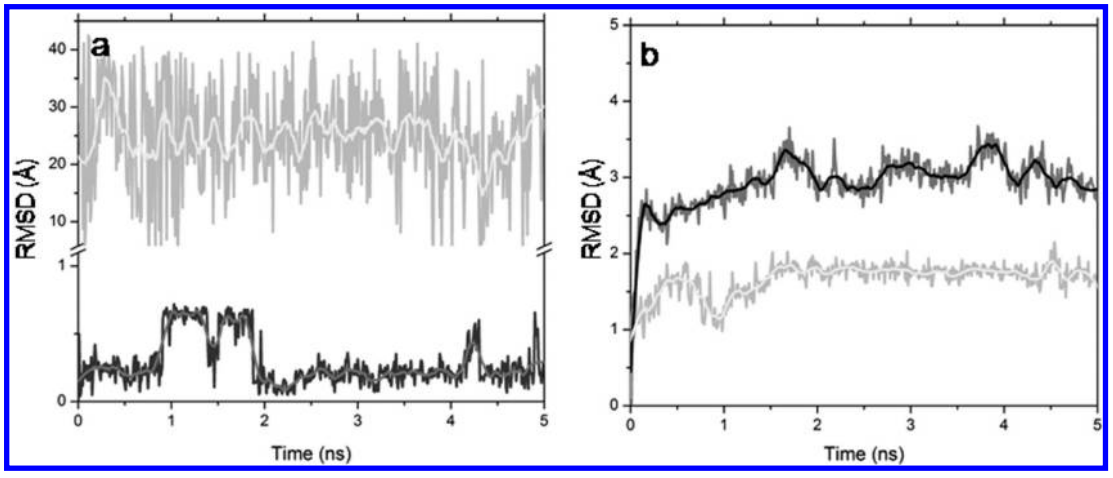

Figure 5. RMSD of the ligand in the best and worst protein−ligand model obtained during 5 ns of MD simulations. (a) Alcohols in the presence of acetyl-CoA as cosubstrate. Interestingly, ethanol (gray line) is unstable with an RMSD around 25 Å, and benzyl alcohol (black line) is most stable with an RMSD around 0.2 Å with a slight increase to 0.5 Å at 1 ns, even when both have the same cosubstrate. (b) Acetyl-CoA in presence of ethanol as cosubstrate (black line) and acetyl-CoA in presence of benzyl alcohol as cosubstrate (gray line); the two substrates are stabilized in the solvent channels with 2.5 and 1.5 Å of RMSD. Representative trajectory after 2 different MD simulations.

complex. In silico studies show that Asp170 is rather involved in the formation of a salt bridge with the conserved Arg294, which is most likely to be important for maintaining the geometry of the active site. Thus, Asp170 does not appear to have a direct role in catalysis, and it is most likely of structural importance, which could explain the reduction of enzyme activity in D170E mutant, as it has been discussed for several other acyltransferases.[28] Furthermore, molecular docking studies showed that the affinity energies of the different Asp170 mutants (D170A, D170N, and D170E) are unfavored (Table 3), and MDS showed the unstable conformation during the molecular dynamics trajectories (Figure 5b) with too long distances between the substrates and the catalytic residues.

Kinetic Mechanism. VpAAT1 catalyzes the acyl transfers to an alcohol and there are two possible kinetic mechanisms for the system: a double-displacement or a ternary complex. To clarify this aspect kinetic study were performed using CoASH as inhibitor (Figure 7). The results indicate a competitive inhibition of CoASH by acetyl-CoA (Figure 7a), and a noncompetitive inhibition by hexanol (Figure 7b). This would indicate that VpAAT1 reaction involves the formation of a ternary complex, the acetyl-CoA-hexanol-VpAAT1 complex prior to the chemical catalysis. It should be mentioned that in a double-displacement mechanism, a noncompetitive inhibition by CoASH toward acetyl-CoA and a competitive inhibition toward hexanol was expected. The ternary complex mechanism agrees with the mechanism described earlier for Ss5MaT1 that catalyzes the transfer of malonyl-CoA.[13]

In addition to that, phylogenetic studies of VpAAT1 showed a closer position to Ss5MaT1 but far from thiolase which could also support this ternary mechanism. Thiolase is an acyl-CoA dependent acyl transferase and uses the double-displacement

dx.doi.org/10.1021/ci400409s | J. Chem. Inf. Model. 2013, 53, 2689−2700

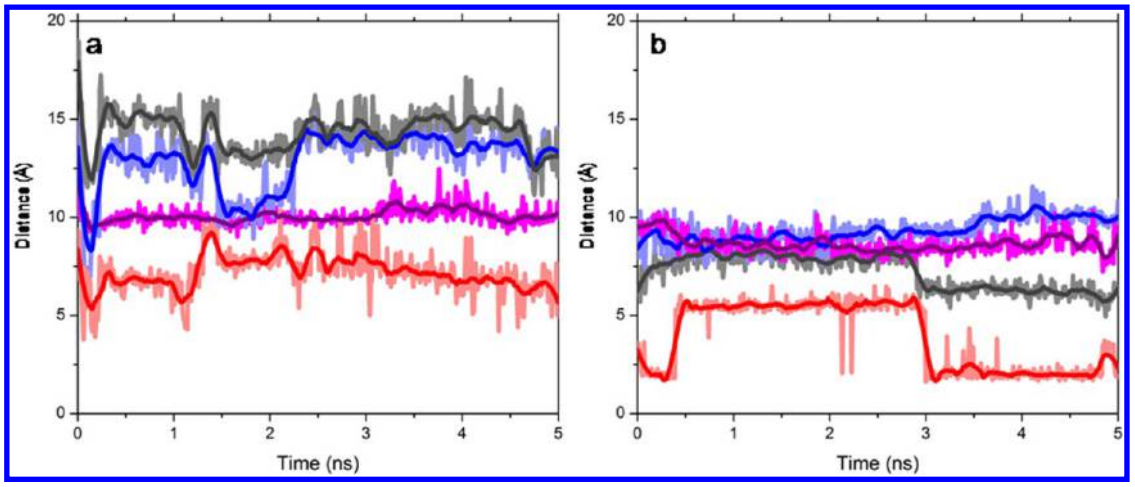

Figure 6. Distance between ligands and active site residues during MD simulation of H166A and D170A. The central line represents 30 FFT smoothing. The purple line show the distance from 166 residue to alcohol, and the red line shows the distance of Ser370 to alcohol. The black line shows the distance of 170 residue to alcohol, and the blue line shows the distance from 166 residue to acetyl-CoA. (a) H166A with benzyl alcohol and acetyl-CoA substrates. A long distance between two substrates and the catalytic residues is observed in all MDS. (b) D170A with benzyl alcohol and acetyl-CoA substrates. A long distance between two substrates and the catalytic residues is observed in all MDS. Representative trajectory after 2 different MD simulations.

Table 4. Kinetic Parameters Obtained for Purified Recombinant VpAAT1 Protein Using the Cosubstrate at a Saturating Concentration[a]

cosubstrate S1 (at variable concentration)	cosubstrate S2 (at saturating concentration)	K_M (μM)		V_{max} (pmol min^{-1})	
ethanol	acetyl-CoA	ND		ND	
butanol	acetyl-CoA	188.6	±2.1	6.0	±0.5
hexanol	acetyl-CoA	157.3	±0.9	5.4	±1.6
benzyl alcohol	acetyl-CoA	133.1	±1.7	31.2	±3.1
acetyl-CoA	benzyl alcohol	75.9	±2.8	31.1	±1.8
acetyl-CoA	hexanol	118.1	±2.0	44.0	±0.6
butanoyl-CoA	hexanol	98.4	±0.9	42.5	±2.1
hexanoyl-CoA	hexanol	91.3	±1.0	33.8	±1.9

[a]ND: The enzyme activity was not measurable (not detected). Data correspond to mean ± SE. Saturating concentrations were 2.5 mM for acetyl-CoA and 4 mM for benzyl alcohol or hexanol. The reaction was initiated by addition of 35 μg purified protein.

mechanism for catalysis,[14] in which a thioester intermediate between the acyl group and a nucleophile (a cysteine residue) is transiently formed prior to the acyl transfer.[13,14] If VpAAT1 operates with the same kind of mechanism as thiolase, an invariant cysteine residue participating in ester linkage formation has to exist in its sequence, and also this Cys should exist on each BAHD family enzyme. However, multiple sequence alignment of BAHD superfamily enzymes do not show the invariant conservation of such residue.[13,29] Therefore, a cysteine-mediated double-displacement mechanism is unlikely for VpAAT1 catalysis.

Taking these lines of evidence together, we propose that the transfer of acyl groups catalyzed by VpAAT1 proceeds with the formation of a ternary complex, as in the case of CAT, HAT, and Ss5MaT1 catalysis.[11−13] To date, the reaction mechanisms and catalytic residues of CAT, HAT, and Ss5MaT1 have been extensively studied in relation to three-dimensional enzyme structures.[11−15,36,37] These enzymes have been shown to share

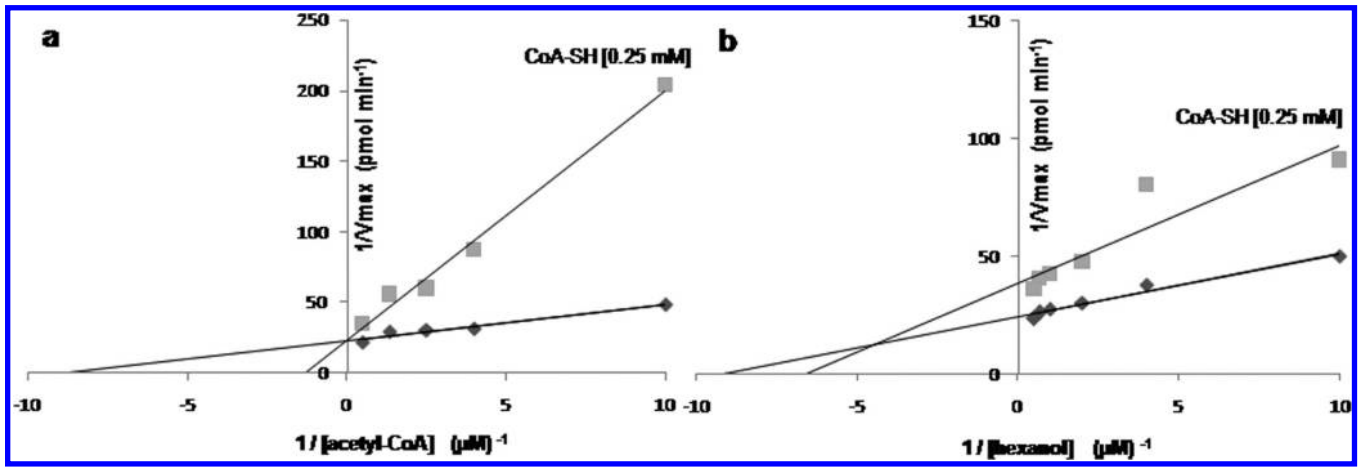

Figure 7. Kinetic analysis of the inhibition of VpAAT1 by coenzyme-A. The data is presented in double-reciprocal plots. (a) Competitive inhibition by CoASH toward acetyl-CoA. Hexanol concentration was fixed at 2.5 mM, and the acetyl-CoA concentrations spanned 0.1 to 2 μM. Enzymatic reactions were performed in the presence of CoASH (0.25 mM) or in its absense. (b) Noncompetitive inhibition by CoASH toward hexanol. Acetyl-CoA concentration was fixed at 0.5 mM, hexanol ranged from 0.1 to 3 μM, and CoASH was set at 0.25 mM.

dx.doi.org/10.1021/ci400409s | J. Chem. Inf. Model. 2013, 53, 2689−2700

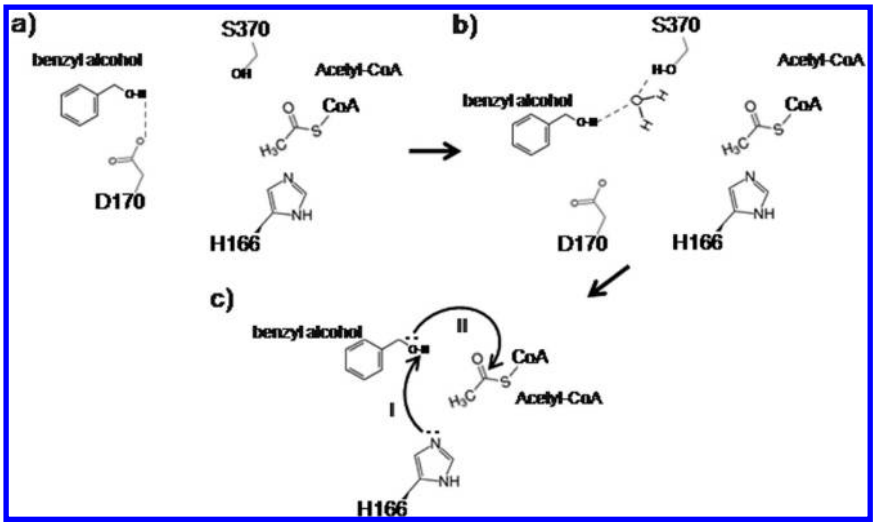

Figure 8. Proposed catalytic mechanism of VpAAT1. (a) Initially, the His166 is oriented to the acetyl-CoA substrate while the Asp170 is oriented to benzyl alcohol. (b) Importance of Ser363 residue and a water molecule in the stability of benzyl alcohol inside the solvent channel. (c) H166 is the base and could deprotonate the hydroxyl of the alcohol (acyl acceptor) to facilitate its nucleophilic attack on the carbonyl carbon of acetyl-CoA. Hydrogen bonds are shown in red dotted lines.

common mechanistic features of acyl transfer: in the ternary complex, a general base activates the nucleophilic group of the acyl acceptor by deprotonation, promoting its nucleophilic attack on the carbonyl carbon of the acyl-CoA. His166 residue should be involved in the general acid/base mechanism of VpAAT1 catalysis.

As we have shown, kinetic studies also agree with the ternary complex mechanism, therefore the VpAAT1 catalytic mechanism should also share such common features with the mechanisms of CAT and HAT. Thus, in the ternary acyl-CoA-alcohol-VpAAT1 complex the H166 is the base and could deprotonate the hydroxyl of the alcohol (acyl acceptor) to facilitate its nucleophilic attack on the carbonyl carbon of acetyl-CoA (Figure.8).

CONCLUSIONS

On the basis of the results presented above, the mutants of VpAAT1 analyzed are less stable than the wild type structure. Only slight differences in overall 3D structure were observed for S34A and H166A compared to wild type. Nevertheless, major changes in shape, volume, and structure were discovered in the solvent channel of D170A and D170N compared to wild type. These changes could explain the unfavored energy of the protein−ligand complex. In the case of D170E, no changes in the solvent channel were observed initially; however during MD trajectory, the solvent channel is narrowed. This could explain the unfavored energy of the protein−ligand complex and the absence of AAT activity in the mutant recombinant protein. The results obtained reveal that the aspartic residue, D170, is important for the maintenance of the solvent channel structure, meanwhile the H166 residue is important for the kinetic mechanism. On the other hand, kinetic analyses indicate that the highest affinity of wild type was against acetyl-CoA (K_M 79.7 μM) and benzyl alcohol (K_M 129.7 μM), coincidence with the values of energy determined for the protein−ligand complex.

The following general mechanism for acyl transfer catalyzed by VpAAT1 enzyme is proposed. The acyl transfer catalyzed by enzymes in the BAHD family of fruits most likely proceeds under a ternary complex mechanism involving the enzyme, the acyl-CoA, and an acyl acceptor. Once the ternary complex is formed, a general base (H166 residue) in the complex promotes the nucleophilic attack of the alcohol on the carbonyl carbon of acyl-CoA.

ASSOCIATED CONTENT

Supporting Information

Affinity energy of different VpAAT1 mutant proteins toward different acyl-CoAs and alcohols as substrates (SI-1) and structural superimposition between VpAAT1-Wt and VpAAT1 mutants (SI-2). This material is available free of charge via the Internet at http://pubs.acs.org.

AUTHOR INFORMATION

Corresponding Author

*Tel.: + 56 71 200 280. Fax: + 56 71 200 276. E-mail address: raherre@utalca.cl.

Author Contributions

L.M.-Q. and M.X.N.-T. performed biochemical experiments. L.M.-Q. performed the structural bioinformatical analysis. L.M.-Q., M.A.M.-L., and R.H. designed the experimental assays and wrote the manuscript.

Notes

The authors declare no competing financial interest.

ACKNOWLEDGMENTS

L.M.-Q. acknowledges CONICYT for a doctoral fellowship. We thank the Center of Bioinformatics and Molecular Simulations (CBSM) of the University of Talca for providing ICM programs. This project was supported by a PBCT Anillo ACT-1110 programme and doctoral thesis grant (AT-2012) (no. 24120932).

REFERENCES

(1) Forney, C. F.; Kalt, W.; Jordan, M. A. The composition of strawberry aroma is influenced by cultivar, maturity and storage. *Hort. Sci.* **2000**, 35, 1022−1026.

(2) Balbontín, C.; Gaete-Eastman, C.; Vergara, M.; Herrera, R.; Moya-León, M. A. Treatment with 1-MCP and the role of ethylene in

aroma development of mountain papaya fruit. *Postharvest Biol. Technol.* **2007**, *43*, 67−77.
(3) Beekwilder, J.; Alvarez-Huerta, M.; Neef, E.; Verstappen, F. W. A.; Bouwmeester, H. J.; Aharoni, A. Functional characterization of enzymes forming volatile esters from strawberry and banana. *Plant Physiol.* **2004**, *135*, 1865−1878.
(4) Dudareva, N.; Pichersky, E.; Gershenzon, J. Biochemistry of plant volatiles. *Plant Physiol.* **2004**, *135*, 1893−1902.
(5) Balbontín, C.; Gaete-Eastman, C.; Fuentes, L.; Figueroa, C. R.; Herrera, R.; Manriquez, D.; Latche, A.; Pech, J. C.; Moya-León, M. A. VpAAT1, A gene encoding an alcohol acyltransferase, is involved in ester biosynthesis during ripening of mountain papaya fruit. *J. Agric. Food Chem.* **2010**, *58*, 5114−5121.
(6) St Pierre, B.; De Luca, V. Evolution of acyltransferase genes: origin and diversification of the BAHD superfamily of acyltransferases involved in secondary metabolism. In *Recent Advances in Phytochemistry Vol. 34. Evolution of Metabolic Pathways*, first ed.; Romeo, J. T., Ibrahim, R., Varin, L., De Luca, V., Eds.; Elsevier Science Ltd: New York, 2000, pp 285−315.
(7) El-Sharkawy, I.; Manriquez, D.; Flores, F. B.; Regad, F.; Bouzayen, M.; Latche, A.; Pech, J. C. Functional characterization of a melon alcohol acyl-transferase gene family involved in the biosynthesis of ester volatiles. Identification of the crucial role of a threonine residue for enzyme activity. *Plant Mol. Biol.* **2005**, *59*, 345−362.
(8) Bayer, A.; Ma, X. Y.; Stockigt, J. Acetyltransfer in natural product biosynthesis - functional cloning and molecular analysis of vinorine synthase. *Bioorg. Med. Chem.* **2004**, *12*, 2787−2795.
(9) Morales-Quintana, L.; Fuentes, L.; Gaete-Eastman, C.; Herrera, R.; Moya-León, M. A. Structural characterization and substrate specificity of VpAAT1 protein related to ester biosynthesis in mountain papaya fruit. *J. Mol. Graphics Modell.* **2011**, *29*, 635−642.
(10) Castrignanò, T.; De Meo, P. D.; Cozzetto, D.; Talamo, I. G.; Tramontano, A. The PMDB Protein Model Database. *Nucleic Acids Res.* **2006**, *34*, D306−D309.
(11) Shaw, W. V.; Leslie, A. G. Chloramphenicol acetyltransferase. *Annu. Rev. Biophys. Biophys. Chem.* **1991**, *20*, 363−386.
(12) Tanner, K. G.; Trievel, R. C.; Kuo, M. H.; Howard, R. M.; Berger, S. L.; Allis, C. D.; Marmorstein, R.; Denu, J. M. Catalytic mechanism and function of invariant glutamic acid 173 from the histone acetyltransferase GCN5 transcriptional coactivator. *J. Biol. Chem.* **1999**, *274*, 18157−18160.
(13) Suzuki, H.; Nakayama, T.; Nishino, T. Proposed mechanism and functional amino acid residues of malonyl-CoA:anthocyanin 5-O-Glucoside-6‴-O-malonyltransferase from flowers of Salvia splendens, a member of the versatile plant acyltransferase family. *Biochemistry* **2003**, *42*, 1764−1771.
(14) Thompson, S.; Mayerl, F.; Peoples, O. P.; Masamune, S.; Sinskey, A. J.; Walsh, C. T. Mechanistic studies on beta-ketoacyl thiolase from *Zoogloea ramigera*: identification of the active-site nucleophile as Cys_{89}, its mutation to Ser_{89}, and kinetic and thermodynamic characterization of wild-type and mutant enzymes. *Biochemistry* **1989**, *28*, 5735−5742.
(15) Rojas, J. R.; Trievel, R. C.; Zhou, J.; Mo, Y.; Li, X.; Berger, S. L.; Allis, C. D.; Marmorstein, R. Structure of tetrahymena GCN5 bound to coenzyme A and a histone H3 peptide. *Nature* **1999**, *401*, 93−98.
(16) Phillips, J. C.; Braun, R.; Wang, W.; Gumbart, J.; Tajkhorshid, E.; Villa, E.; Chipot, C.; Skeel, R. D.; Kale, L.; Schulten, K. Scalable molecular dynamics with NAMD. *J. Comput. Chem.* **2005**, *26*, 1781−1802.
(17) MacKerell, A. D., Jr.; Bashford, D.; Bellott, M.; Dunbrack, R. L., Jr.; Evanseck, J.; Field, M.; Fischer, J. S.; Gao, J.; Guo, H.; Ha, S.; Joseph, D.; Kuchnir, K.; Kuczera, L.; Lau, F. T. K.; Mattos, C.; Michnick, S.; Ngo, T.; Nguyen, D. T.; Prodhom, B.; Roux, B.; Schlenkrich, M.; Smith, J.; Stote, R.; Straub, J.; Watanabe, M.; Wiorkiewicz-Kuczera, J.; Yin, D.; Karplus, M. Self-consistent parameterization of biomolecules for molecular modeling and condensed phase simulations. *FASEB J.* **1992**, *6*, A143.
(18) Schlenkrich, M.; Brickmann, J.; MacKerell, A. D.Jr.; Karplus, M. A molecular perspective from computation and experiment. In *Biological Membranes A molecular perspective from computation and experiment*, first ed.; Merz, K. M., Roux, B., Eds.; Birkhauser: Boston, MA, 1996; pp 31−81.
(19) Jorgensen, W. L.; Chandresekhar, J.; Madura, J. D.; Impey, R. W.; Klein, M. L. Comparison of simple potential functions for simulating liquid water. *J. Chem. Phys.* **1983**, *79*, 926−935.
(20) Abagyan, R.; Totrov, M.; Kuznetsov, D. ICM- A new method for protein modeling and design: Applications to docking and structure prediction from the distorted native conformation. *J. Comput. Chem.* **1994**, *15*, 488−506.
(21) Vanommeslaeghe, K.; Hatcher, E.; Acharya, C.; Kundu, S.; Zhong, S.; Shim, J.; Darian, E.; Guvench, O.; Lopes, P.; Vorobyov, I.; MacKerell, A. D., Jr. CHARMM General Force Field: A Force field for Drug-Like Molecules Compatible with the CHARMM All-Atom Additive Biological Force Field. *J. Comput. Chem.* **2010**, *31*, 671−690.
(22) Humphrey, W.; Dalke, A.; Schulten, K. VMD Visual molecular dynamics. *J. Mol. Graph.* **1996**, *14*, 33−38.
(23) Bradford, M. M. A rapid and sensitive method for the quantification of microgram quantities of protein utilizing the principle of protein dye binding. *Anal. Biochem.* **1976**, *72*, 248−254.
(24) Fellman, J. K.; Mattinson, D. S.; Bostick, B. C.; Mattheis, J. P.; Patterson, M. E. Ester biosynthesis in 'Rome' apples subjected to low oxygen atmospheres. *Postharvest Biol. Technol.* **1993**, *3*, 201−214.
(25) González, M.; Gaete-Eastman, C.; Valdenegro, M.; Figueroa, C. R.; Fuentes, L.; Herrera, R.; Moya-León, M. A. Aroma development during ripening of *F. chiloensis* fruit and participation of an alcohol acyltransferase (FcAAT1) gene. *J. Agric. Food Chem.* **2009**, *57*, 9123−9132.
(26) Kemmer, G.; Keller, S. Nonlinear least-squares data fitting in Excel spreadsheets. *Nat. Protoc.* **2010**, *5*, 267−281.
(27) D'Auria, J. C. Acyltransferases in plants: a good time to be BAHD. *Curr. Opin. Plant Biol.* **2006**, *9*, 331−340.
(28) Ma, X.; Koep, J.; Panjikar, S.; Fritzch, G.; Stockigt, J. Crystal structure of vinorine synthase, the first representative of the BAHD superfamily. *J. Biol. Chem.* **2005**, *280*, 13576−13583.
(29) Morales-Quintana, L.; Moya-León, M. A.; Herrera, R. Molecular docking simulation analysis of alcohol acyltransferases from two related fruit species explains their different substrate selectivities. *Mol. Simul.* **2012**, *38*, 912−921.
(30) Wu, D.; Govindasamy, L.; Lian, W.; Gu, Y.; Kukar, T.; Agbandje-McKenna, M.; McKenna, R. Structure of human carnitine acetyltransferase: molecular basis for fatty acyl transfer. *J. Biol. Chem.* **2003**, *278*, 13159−13165.
(31) Galaz, S.; Morales-Quintana, L.; Moya-León, M. A.; Herrera, R. Structural analysis of the alcohol acyltransferase protein family from *Cucumis melo* shows that enzyme activity depends on an essential solvent channel. *FEBS J.* **2013**, *280*, 1344−1357.
(32) Yahyaoui, F.; Wongs-Aree, C.; Latché, A.; Hackett, R.; Grierson, D.; Pech, J. C. Molecular and biochemical characteristics of a gene encoding an alcohol acyl-transferase involved in the generation of aroma volatile esters during melon ripening. *Eur. J. Biochem.* **2002**, *269*, 2359−2366.
(33) Olías, R.; Pérez, A. G.; Sanz, C. Catalytic properties of alcohol acyltransferase in different strawberry species and cultivars. *J. Agric. Food Chem.* **2002**, *50*, 4031−4036.
(34) Olías, J. M.; Sanz, C.; Ríos, J. J.; Pérez, A. G. Substrate specificity of alcohol acyltransferase from strawberry and banana fruits. *ACS Symp. Ser.* **1995**, *596*, 134−141.
(35) Wyllie, G.; Fellman, J. Formation of volatile branched chain esters in bananas (*Musa sapientum* L.). *J. Agric. Food Chem.* **2000**, *48*, 3493−3497.
(36) Leslie, A. G. Refined crystal structure of type III chloramphenicol acetyltransferase at 1·75 Å resolution. *J. Mol. Biol.* **1990**, *213*, 167−186.
(37) Lewendon, A.; Murray, I. A.; Shaw, W. V. Replacement of catalytic histidine-195 of chloramphenicol acetyltransferase: Evidence

for a general base role for glutamate. *Biochemistry* **1994**, *33*, 1944−1950.